

Ion implantation in silicon for trimming the operating wavelength of ring resonators

Milan M. Milosevic¹, Xia Chen¹, Wei Cao¹, Antoine F. J. Runge¹, Johann Franz¹, Callum G. Littlejohns^{1,2}, Sakellaris Mailis¹, Anna C. Peacock¹, David J. Thomson¹, Graham T. Reed¹

¹*Optoelectronics Research Centre, University of Southampton, UK*

²*Silicon Technologies Centre of Excellence, Nanyang Technological University, Singapore*

Abstract— In recent years, we have presented results on the development of erasable gratings in silicon to facilitate wafer scale testing of photonics circuits via ion implantation of germanium. Similar technology can be employed to control the operating wavelength of ring resonators, which is very sensitive to fabrication imperfections. Ion implantation into silicon causes radiation damage resulting in a refractive index increase, and can therefore form the basis of multiple optical devices. In this paper we discuss design, modelling and fabrication of ring resonators and their subsequent trimming using ion implantation of germanium into silicon, followed by either rapid thermal annealing or localized laser annealing. The results confirm the ability permanently tune the position of the resonant wavelength to any point inside the free spectral range of the ring resonator, thus greatly reducing the amount of power required for active tuning of these devices.

Index Terms—Ion implantation, laser annealing, optical interconnects, rapid thermal annealing, ring resonators, silicon photonics, trimming.

I. INTRODUCTION

Silicon photonics, pioneered as a material platform for thirty years, is at present one of the most buoyant technologies in the world, and is particularly regarded as a low cost solution for short reach interconnects for applications in the information and communication sectors, environmental engineering, and healthcare [1]-[10]. The technology is able to make use of the large silicon manufacturing infrastructure already in existence for the microelectronics industry, positioning itself at the threshold many the mass markets.

The ring resonator represents one of the basic building blocks of many photonic circuits. It is widely used for both active and passive devices, and has been used in particular for the development of a number of applications such as lasing, filtering, modulation and sensing, aiming to provide devices that offer compactness and low power consumption. However, it is very challenging to achieve precise control of positioning and stability of the resonant wavelength peak of a micro-ring resonator due to its high sensitivity to fabrication errors and environmental changes. A heater or thermoelectric cooler is

typically used to trim and actively control the position of the resonant wavelength peak. However, this requires additional power consumption and control complexity which are some of the key obstacles to development of viable commercial optoelectronic products. Standard configurations in which deposited oxide (~1 μm) separates the waveguide and a metal heater revealed tuning efficiencies between 42 mW/FSR and 100 mW/FSR (FSR - free spectral range) [5]. Conversely, thermal isolation of the resonant structure from the silicon substrate may be used to obtain an order of magnitude improvement in tuning efficiency (2.4 - 4.9 mW/FSR) [5], while introduction of transparent graphene nanoheaters suggests promising prospects for further improvements in heating efficiency (~0.48 nm/mW) together with the device footprint [6]. The fabrication process and silicon-on-insulator (SOI) wafer thickness variations induce similar or perhaps even larger resonant wavelength shift than environmental changes, thus requiring high power consumption to rectify the operating wavelength error. Therefore, post-fabrication trimming of the ring resonator has been investigated by researchers worldwide. For example, electron beam induced compaction and strain to the oxide cladding have been proposed as methods to trim the resonant wavelength peak of silicon ring resonators [8]. However, in this case the refractive index variation of the oxide is quite small, which limits the tuning range (resonant wavelength red shift of up to 4.9 nm was observed). Additionally, it is an expensive and comparatively slow process. Electron beam bleaching of a polymer cladding was also proposed for more effective trimming [9] but it lacks universal CMOS compatibility, and is a similarly slow process.

Ion implantation into silicon causes radiation damage. If a sufficient dose is implanted, complete amorphisation can be realised in the implanted part of the device. Amorphous silicon has a refractive index that is significantly different (higher) than that of crystalline silicon (by approximately 10^{-1} refractive index units), and can therefore form the basis of multiple optical devices. In previous work by Ackert et al. [10], silicon ion implantation was used for tuning the resonant wavelength of racetrack ring resonators up to ~3 nm. However, high optical loss, poor extinction ratio and low Q-factor were reported. In

Manuscript received June 14, 2017.

M. M. Milosevic, X. Chen, W. Cao, Antoine F. J. Runge, Y. Franz, C. G. Littlejohns, S. Mailis, A. C. Peacock, D. J. Thomson and G. T. Reed are with the Optoelectronics Research Centre, University of Southampton, UK (e-mail: m.milosevic@soton.ac.uk, xia.chen@soton.ac.uk, wei.cao@soton.ac.uk, a.f.runge@soton.ac.uk,

y.franz@soton.ac.uk, c.littlejohns@soton.ac.uk, sm@orc.soton.ac.uk, acp@orc.soton.ac.uk, d.thomson@soton.ac.uk, g.reed@soton.ac.uk).

C. G. Littlejohns is also with Silicon Technologies Centre of Excellence, Nanyang Technological University, Singapore.

this paper, we have implemented germanium ion implantation based refractive index change in a selection of integrated photonic devices, focusing on resonant structures, although application to any optical device is possible. Germanium ions have been chosen in order to achieve a good amorphisation profile at a relatively low implantation dose ($\sim 10^{15}$ ions/cm²) thus reducing the processing time and costs. Furthermore, if compared to common doping ion species, Germanium is a CMOS compatible material and the implantation process can be carried out at room temperature without self-annealing of the amorphous material during the implantation phase [1]. This reversible refractive index change can be selectively removed by selective local annealing to tune the operating wavelength of the device. As discussed earlier, the total power consumption required for active tuning of the resonant wavelength peak position consists of two parts: the power required to compensate for the resonant wavelength shift caused by fabrication process and the power required to compensate for the temperature dependent wavelength shift caused by environmental changes. We believe that most photonic chips with ring resonators will have a designed working temperature, which will be controlled by an external thermal system. Using Ge-ion implantation approach, we can trim the operating wavelength to a target wavelength at the designed working temperature, in order to reduce the power consumption required for thermal tuning. In this paper, we discuss this approach in the context of active device trimming.

II. DESIGN AND FABRICATION

Any resonant wavelength shift in a ring resonator depends on the mode effective index and the optical path length at the wavelength of interest [3]. The mode effective index at a given temperature depends on the material refractive index, waveguide dimensions, and operating wavelength. We have used Lumerical software [11] for simulation analysis. Standard SOI rib waveguides with 220 nm crystalline silicon height (100 nm silicon slab layer) and a 2 μm buried oxide layer have been used. For all 500 nm wide silicon waveguides, we have designed and fabricated ring resonators with $R=10\ \mu\text{m}$ radius, an edge-to-edge waveguide spacing of $\text{Gap}=120\ \text{nm}$ and different implantation arc lengths $\theta = (2^\circ, 6^\circ, 10^\circ, 14^\circ, 18^\circ, 22^\circ)$ (Fig. 1). Un-implanted ring resonators with the same dimensions were also fabricated for reference.

The layout of the Ge implanted section is shown in Fig. 1b. The arc length of the ion implanted section is denoted by angle θ . The width of ion implanted region, located in the center of silicon rib waveguide, was equal to 400 nm. A short taper, with a tip width of 120 nm, was formed at both ends of the ion implanted region ($\theta_{\text{tap}}=5^\circ$), in order to reduce both reflection of light between the silicon and Ge ion implanted regions of the waveguide, and potential resonance inside the ion implanted waveguide section. Rib waveguides and ring resonators were fabricated by electron beam lithography and inductively coupled plasma etching. After resist removal, a 20 nm thick PECVD oxide was deposited as a protective layer. Next, an electron beam resist layer was deposited as a mask layer for Ge ion implantation. An ion energy and fluence of 130 KeV and 1×10^{15} ions/cm² were used, respectively. According to our previously results [1], [2], this will provide 80% lattice disorder

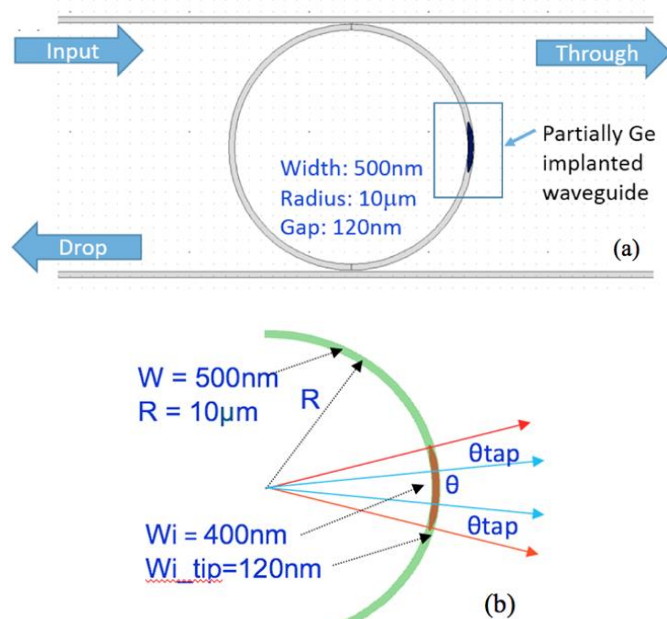


Fig. 1: (a) A schematic of a ring resonator with a section of amorphous silicon created by germanium ion implantation. (b) A detailed layout of the germanium ion implanted waveguide section.

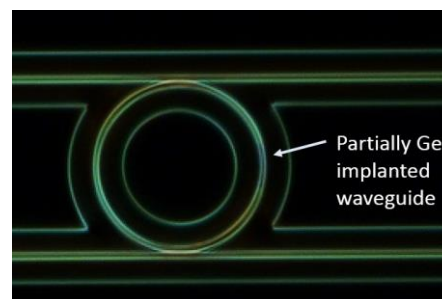


Fig. 2: An optical microscope image of the fabricated ring resonator with a partially ion implanted Ge waveguide section.

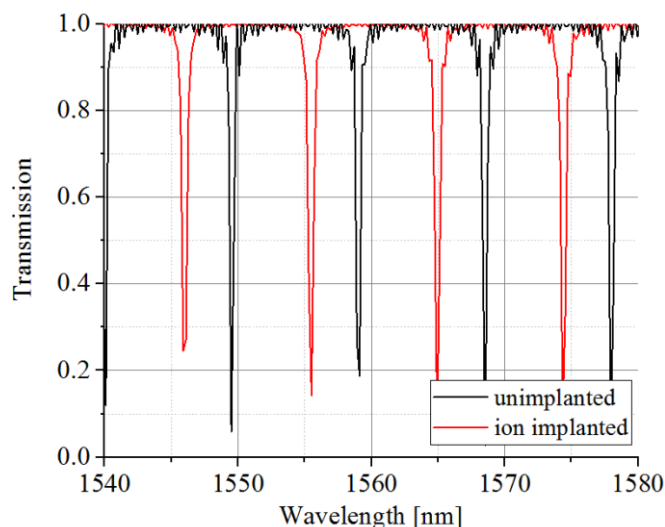


Fig. 3: Simulation results of implanted devices showing a transmission spectrum of an un-implanted and Ge ion implanted ring resonator ($\theta=6^\circ$).

in silicon with a refractive index change of 0.5. The refractive index profile was measured using ellipsometry on a bulk implanted substrate, at 6 different angles of incidence as described in detail in Ref. [1]. It is found to be 3.96 (at 1550 nm) after Ge-ion implantation, and this value was used in our simulation analysis. The germanium ion concentration, implanted into silicon, was negligible to the concentration of silicon ions in the same volume (up to 0.3% at its peak value). An optical microscope image of a fabricated ring resonator is shown in Fig. 2. Simulation results, showing the transmission spectrum of an un-implanted and Ge ion implanted ring resonator ($\theta=6^\circ$), are presented in Fig. 3. As it can be seen, the resonant wavelength shifts to longer wavelengths due to greater mode interaction with the amorphous silicon.

III. EXPERIMENTAL RESULTS

A tunable laser with a wavelength range from 1520 to 1620 nm was used to characterize the fabricated devices. To accurately measure the output signal, we used a sample stage with a Peltier element to keep the temperature constant during measurements (20 °C). Shallow etched (70 nm) gratings optimized for TE polarization were used at the input/output of the waveguide to provide efficient coupling of light from/to the single-mode optical fibers used for testing. The results presented in this paper are for wavelengths around $\lambda \sim 1550$ nm. However, similar results have been obtained at other wavelengths.

Fig. 4a shows a typical transmission spectrum comparing the performance of an un-implanted ring resonator and Ge ion implanted ring resonators with various implantation lengths. The resonant wavelength peak of an un-implanted ring resonator revealed resonant wavelengths at around 1561 nm and 1571 nm. The results showed good agreement with simulation analysis (Fig. 3). A difference within 2 nm in the target wavelength peak position before (~ 1559 nm simulated, ~ 1561 nm measured) and after (~ 1565 nm simulated, ~ 1566 nm measured, $\theta=6^\circ$) Ge-ion implantation can be associated to fabrication process and SOI wafer thickness variations. A clear trend of the resonant wavelength shift was observed for implanted resonators. The resonant wavelength shifts to longer wavelengths as implantation length is increased due to greater mode interaction with the amorphous silicon. Measured ring resonators exhibited an extinction ratio of over 20 dB in all cases and a similar spectral shape. It is worth mentioning that the measured devices were very close to each other on the same chip thus keeping the SOI wafer thickness variations and fabrication difference between each device to a minimum. Additionally, an electron beam lithography tool, used for device fabrication, provided very high accuracy lithography and therefore small device width variations. However, we were unable to establish a precise theoretical relationship between the implantation length and the resonant wavelength shift, because the data were collected from different ring resonators, although at the same location on the wafer. The resonant wavelengths will be greatly affected by the fabrication process. A wavelength shift of ~ 0.6 nm per micron of implanted waveguide can be estimated. Devices carrying the same design parameters (and implantation length) may have up to 3 nm difference in the resonant wavelength according to our

measurement, even if they are located next to each other on the same chip of the wafer. This also proves high sensitivity of these devices to fabrication process and wafer properties and hence a need for post-fabrication trimming. With our proposed technique, these resonators can still be trimmed to the desired resonant wavelength. The results also showed that ion implanted waveguide sections only induced a very small amount of loss (<0.2 dB), which didn't degrade the overall performance of ring resonators significantly.

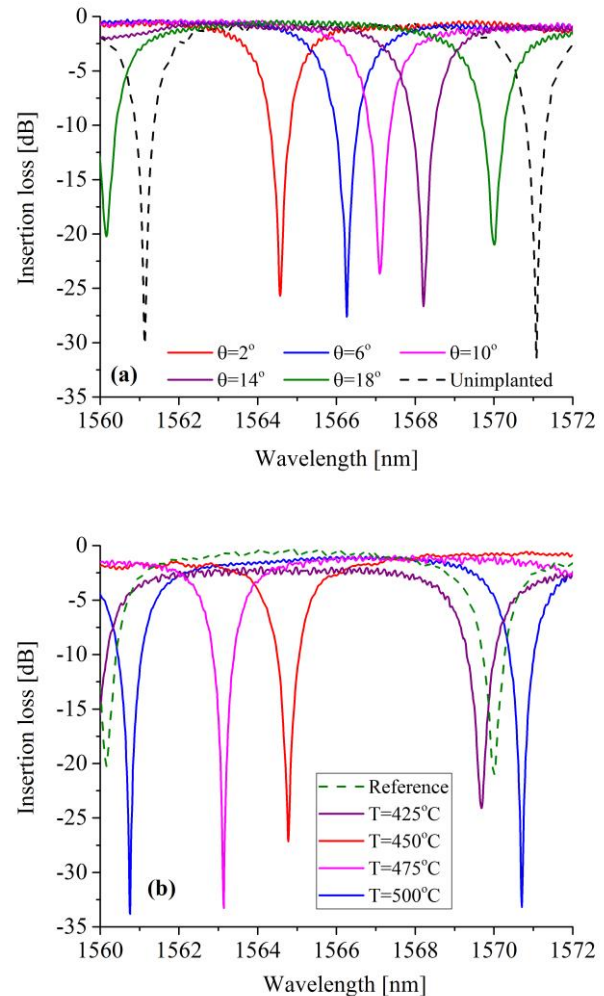


Fig. 4: Transmission spectra of fabricated ring resonators. (a) As implantation length increases resonant wavelength peak shifts to longer wavelengths (un-annealed samples). (b) As annealing temperatures increases the resonant wavelength peak shifts to shorter wavelengths ($\theta=18^\circ$).

A. Rapid thermal annealing (RTA)

The refractive index of implanted silicon is about 3.96, which could be gradually reduced to 3.47 by cycles of rapid thermal annealing (RTA) due to re-crystallisation of the implanted silicon [1]. It can be additionally controlled by adjusting the annealing time, thus shifting the resonant wavelength to a chosen target position. Therefore, a one minute RTA was carried out to partially anneal the implanted silicon regions at different temperatures, in order to characterize the trimming

process. It was found that an annealing temperature below 250°C caused essentially no change in the position of the resonant wavelength. However, at higher temperatures a clear blue shift was observed. Fig. 4b shows the comparison of the transmission spectrum between an un-implanted ring resonator and the implanted ring resonator ($\theta=18^\circ$) at different annealing temperatures of 425, 450, 475, and 500 °C, respectively. The FWHM of those spectra are 1.67 nm (Reference), 1.64 nm (425 °C), 1.58 nm (450 °C), 1.49 nm (475 °C) and 1.45 nm (500 °C) which corresponded to a Q-factor of 940, 957, 990, 1049 and 1076. It can be seen that the Q factor increased as annealing temperature was increased, showing a reduction of the round-trip loss of the ring cavity by applying the thermal annealing technique. Measured results revealed a material absorption loss of 0.03 dB/ μm . Propagation losses of Ge-ion implanted waveguides were ~ 32 dB/mm before annealing. The origin of the loss is the amorphisation of the crystal, not the germanium concentration. This result is in a good agreement with measured Q-factor of our resonators. After performing partial annealing of ion implanted section, we measured waveguide propagation losses of less than 10 dB/mm, and for fully annealed waveguides we didn't obtain any significant difference in propagation losses compared to a standard unimplanted rib waveguide, demonstrating that the germanium is not the origin of the loss, and that, in fact, the dose is very low at 0.3%. The highest quality factor of our rings was in the range of 1000-1500 after annealing which is in a good agreement with the Q factor of unimplanted ring resonator (~ 1400). The low-quality factors of our ring resonators are associated with the presence of a drop-port in our initial design. The germanium ion concentration, implanted into silicon, was negligible compared to the concentration of silicon ions in the same volume (up to 0.3% at its peak value as previously stated) and had a negligible effect on the Q-factor.

Fig. 5 shows the resonant wavelength shift for various implantation lengths and annealing temperatures of 425, 450, 475, and 500 °C, respectively. The effective length of the ion implanted waveguide region was calculated to include ion implanted tapers on both ends of the ion implanted region of the waveguide. A linear relationship between the resonant wavelength shift and implantation length was observed in all cases as expected. The shift was very low at low annealing temperatures and it increased at higher temperatures due to change in refractive index of the implanted region. It can be seen that an implantation length of 6 μm would provide a resonant wavelength shift of 10 nm, which corresponds to the free spectral range of the fabricated ring resonators. Therefore, we need to make one additional lithographic mask during device fabrication to perform Ge-ion implantation to obtain this implantation length and then use our annealing technique to trim the operating wavelength. For practical applications, the trimming of individual rings can also be done by localized laser annealing which is explored in the next section of this paper.

Trimming stability experiments of implanted ring resonators were also performed (Fig. 6). The samples were left in an oven at 220°C for one day (24 hours) and then a further week. The resonator wavelength shift followed the same trend as before, the wavelength shift increased for longer implantation lengths, however the maximum resonance shift was small (0.38 nm during a period of 8 days at 220°C).

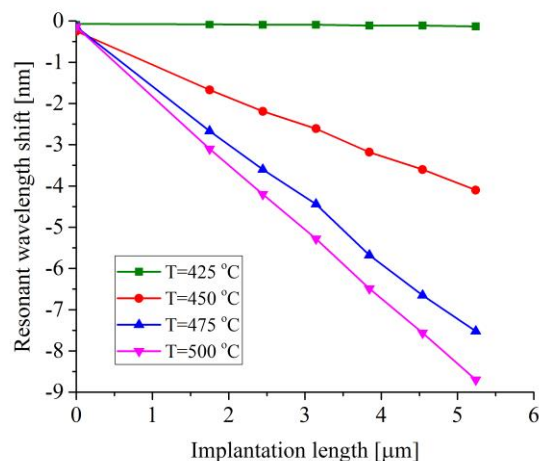


Fig. 5: Changes in resonant wavelength shift as a function of implantation length at different annealing temperatures.

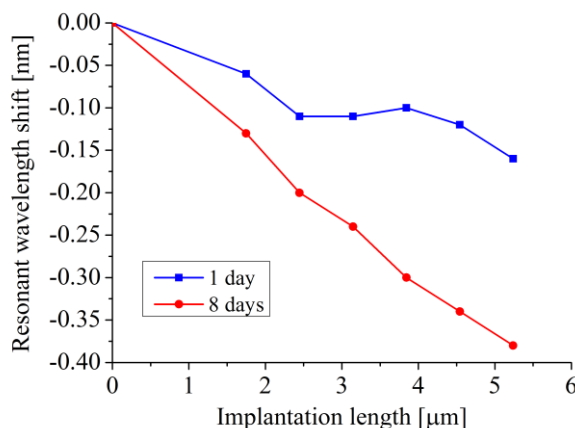


Fig. 6: Trimming stability of implanted ring resonators. Changes in resonant wavelength as a function of implantation length, whilst held at an elevated temperature of 220 °C during a period of up to 8 days.

B. Localised laser annealing

The laser annealing setup shown in Fig. 7 is similar to the one described in Ref. [12] and was designed to deliver 488 nm continuous wave Argon ion laser power to the amorphous silicon in a controlled and precise manner (Fig. 7). Continuous wave lasers have been shown to produce larger silicon crystal grain sizes with fewer defects than those obtained by pulsed sources, resulting in a qualitative improvement in recrystallization of amorphous silicon, thus obtaining higher material quality [13]. This is attributed to the lower cooling rate after laser irradiation from continuous wave sources. The output power was adjusted using a half wave plate and a polarization cube splitter. The laser beam was focused on the sample top surface using a 10x microscope objective, producing a 4.7 μm diameter spot. The sample was scanned under the laser beam using a set of linear micro-precision linear stages while a pellicle beam splitter and a CCD camera were used for imaging and control. Using the correct combination of laser power and scanning speed, sufficient thermal energy was transferred to the

amorphous Silicon material to partially re-crystallize the Si material, thus modifying its optical properties.

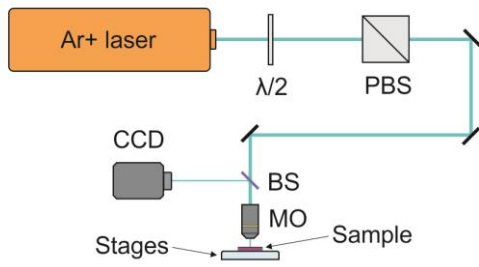


Fig. 7: Experimental laser annealing setup (PBS - polarization beam splitter; BS - pellicle beam splitter; MO - microscope objective).

Fig. 8 shows the resonant wavelength shift before and after localized laser annealing for an implantation arc length of $\theta=18^\circ$ and a laser power of approximately 90 mW. Similar to our previous results (Fig. 4a), the resonant wavelength peak of an un-implanted ring resonator revealed resonant wavelengths at around 1563.5 nm and 1573.5 nm, respectively. Small variations in the target wavelength peak of around ~ 2.8 nm can be associated to the SOI wafer thickness variations and fabrication errors. Once again this confirmed the high sensitivity of these devices to any imperfections, and hence the need for trimming. In fact, the variation of 2.8-nm in target operating wavelength is comparable to the resonant wavelength shift caused by environmental changes. It corresponds to a temperature change of $\Delta T=28-47$ K assuming a typical temperature dependent resonant wavelength shift between 60 and 100 pm/K, respectively [3]. As it can be seen from Figure 8, a clear blue shift of around 7 nm was observed. This corresponds to several milliwatts of power required to actively tune these devices.

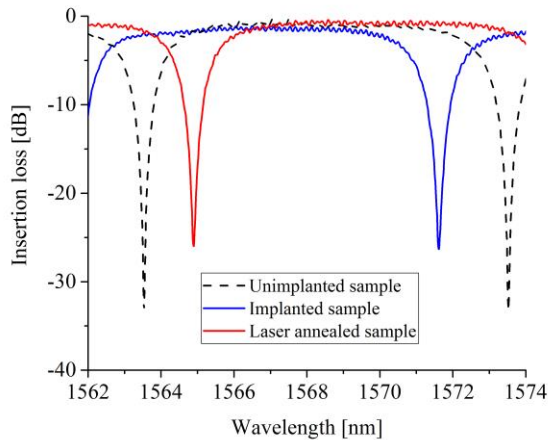


Fig. 8: Transmission spectra of fabricated ring resonators before and after laser annealing ($\theta=18^\circ$).

We performed a series of experiments by varying the laser power to monitor the resonant wavelength shift of fabricated ring resonators. Fig. 9 shows changes in resonant wavelength shift per implanted length as a function of laser power used for localized annealing. A laser power between 60–95 mW is sufficient to provide positioning of the resonant wavelength

peak at any place inside the free spectral range of the ring resonator for a given implantation length. As it can be seen from Figure 9, the resonant wavelength shift is very sensitive between 80-85 mW and will require precise control in order to achieve the desired resonance shift.

Table I shows a comparison between our technique and the state of the art results obtained from the literature. As it can be seen, Ge-ion implantation followed by localised laser annealing is a relatively fast process (processing time ~ 0.5 h/wafer) allowing a high throughput which is very important for industrial applications. It is several times faster than electron beam methods and an order of magnitude cheaper. The process is CMOS compatible and demonstrates the ability to permanently adjust the resonant wavelength peak position to a target wavelength within any position across the free-spectral range of the fabricated ring resonator.

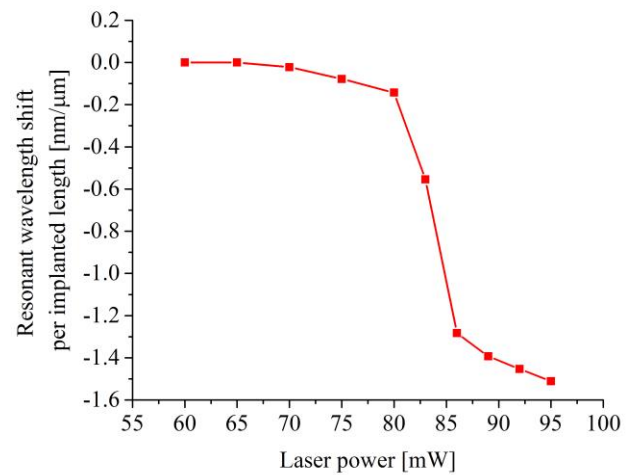


Fig. 9: Changes in resonant wavelength shift per implanted length as a function of laser power used for localized annealing.

Table I: Comparison with the current state of the art of trimming of ring resonators.

Parameter/Reference	Ref. [8]	Ref. [9]	This paper
CMOS compatibility	Yes	No	Yes
Throughput (hours/wafer)	Low (>8)	Low (>8)	High (<0.5)
Costs (GBP/wafer)	High (~10,000)	High (~10,000)	Low (<1,000)
Trimming range (nm)	4.91	2	10

IV. CONCLUSION

We performed simulation and experimental analysis on trimming the position of the resonant wavelength peak of silicon ring resonators due to a resonant wavelength shift caused by fabrication process. Partial rapid thermal annealing

and localized laser annealing of the ion implanted section revealed the ability to permanently adjust the resonant wavelength peak position to a target wavelength, and therefore reduce the relatively high power consumption (typically tens of milliwatts) required to precisely control the operating wavelength. The RTA process gives us much more information about the required temperature vs annealing process than the local laser annealing, but local annealing is required for practical applications so that the remainder of the optical circuit is not affected. The process is CMOS compatible and can be transferred to other platforms and systems such as multilayer photonics and programmable photonic circuits.

ACKNOWLEDGMENT

This work was funded by EPSRC project under the “Silicon Photonics for Future Systems”, “Electronic-Photonic convergence”, “Laser-Engineered Silicon” and “CORNERSTONE” projects. Reed is a Royal Society Wolfson Research Merit Award holder. He is grateful to the Wolfson Foundation and the Royal Society for funding of the award. Thomson acknowledges funding from the Royal Society for his University Research Fellowship. CGL acknowledges funding from National Research Foundation of Singapore (NRF-CRP12-2013-04).

References

1. R. Topley, L. O’Faolain, D. J. Thomson, F. Y. Gardes, G. Z. Mashanovich, and G. T. Reed, “Planar surface implanted diffractive grating couplers in SOI,” *Opt. Express*, vol. 22, pp. 1077-1084, 2014.
2. R. Topley, G. Martinez-Jimenez, L. O’Faolain, N. Healy, S. Mailis, D. J. Thomson, F. Y. Gardes, A. C. Peacock, D. N. R. Payne, G. Z. Mashanovich, and G. T. Reed, “Locally erasable couplers for optical device testing in silicon on insulator,” *Journal of Lightw. Technol.*, vol. 32, no. 12, pp. 2248-2253, 2014.
3. M. M. Milosevic, N. G. Emerson, F. Y. Gardes, X. Chen, A. A. D. T. Adikaari, G. Z. Mashanovich, “Athermal waveguides for optical communication wavelengths,” *Opt. Lett.*, vol. 36, no. 23, pp. 4659-4651, 2011.
4. G. T. Reed, G. Mashanovich, F. Y. Gardes, D. J. Thomson, “Silicon optical modulators,” *Nat. Photon.*, vol. 4, pp. 518-526, 2010.
5. K. Padmaraj, K. Bergman, “Resolving thermal challenges for silicon microring resonator devices,” *Nanophoton.*, vol. 3, no. 4-5, pp. 269-281, 2014.
6. L. Yu, Y. Yin, Y. Shi, D. Dai, S. He, “Thermally tunable silicon photonic microdisk resonator with transparent graphene nanoheaters,” *Optica*, vol. 3, no. 2, pp. 159-166, 2016.
7. W. Bogaerts, P. De Heyn, T. Van Vaerenbergh, K. De Vos, S. K. Selvaraja, T. Claes, P. Dumon, P. Bienstman, D. Van Thourhout, and R. Baets, “Silicon microring resonators,” *Laser Photon. Rev.*, vol. 6, pp. 47-73, 2012.
8. J. Schrauwen, D. Van Thourhout, and R. Baets, “Trimming of silicon ring resonator by electron beam induced compaction and strain,” *Opt. Express*, vol. 16, pp. 3738-3743, 2008.
9. S. Prorok, A. Y. Petrov, M. Eich, J. Luo, and A. K.-Y. Jen, “Trimming of high-Q-factor silicon ring resonators by electron beam bleaching,” *Opt. Lett.*, vol. 37, pp. 3114-3116, 2012.
10. J. J. Ackert, J. K. Doylend, D. F. Logan, P. E. Jessop, R. Vafaei, L. Chrostowski, A. P. Knights, “Defect-mediated resonance shift of silicon-on-insulator racetrack resonators,” *Opt. Express*, vol. 19, no. 13, pp. 11970-11976, 2011.
11. www.lumerical.com
12. N. Healy, S. Mailis, N. M. Bulgakova, P. J. A. Sazio, T. D. Day, J. R. Sparks, H. Y. Cheng, J. V. Badding, and A. C. Peacock, “Extreme electronic bandgap modification in laser-crystallized silicon optical fibres,” *Nat. Mater.*, vol. 13, pp. 1122-1127, 2014.
13. K. Kitahara, Y. Ohashi, Y. Katoh, A. Hara, and N. Sasaki, “Submicron-scale characterization of poly-Si thin films crystallized by excimer laser and continuous-wave laser,” *Journal of Appl. Phys.*, vol. 95, pp. 7850-7855, 2004.

Milan M. Milosevic: Milan Milosevic is a research fellow at the Optoelectronics Research Centre, University of Southampton, working on both industry and research council funded projects, led by Prof. Graham Reed. Previously he was working as an engineer and technology consultant in the US and Japan, and as a research fellow at the University of Surrey where he also obtained his PhD degree and received the Vice-Chancellor’s Award for Early Career Excellence in 2012. He is particularly involved in high speed optical transceiver technology and is one of the pioneers in mid-infrared silicon photonics technology for emerging applications.

Xia Chen: Xia Chen is a senior research fellow at Optoelectronics Research Centre, University of Southampton. He received B.Eng. and Ph.D. degrees in Electronics Engineering from the Chinese University of Hong Kong in 2006 and 2010, respectively. After graduation, he worked on the UK Silicon Photonic Project in University of Surrey and University of Southampton. In 2013, he joined Huawei Technologies Co. Ltd as a senior engineer to work on photonic packaging. He rejoined the Silicon Photonics group in University of Southampton in 2015. He was awarded the TSMC Outstanding Student Research Award in 2010, and the Newton International Fellowship by the Royal Society in 2011. He has authored and coauthored over 70 papers in technical journals and international conferences and 4 patents.

Wei Cao: Wei Cao is a PhD student in the Silicon Photonics group at the Optoelectronics Research Centre (ORC) in the University of Southampton. He is current developing high speed modulator using group IV material in the mid-infrared wavelength, under the supervision of Prof Goran Mashanovich and Prof Graham Reed. He obtained M.Sc. of Photonics Technologies at the ORC in the University of Southampton, as the top student in the cohort. He accomplished M.Eng. and B.Eng. of Electrical and Electronics Engineering (EEE) in the Imperial College London.

Antoine F. J. Runge: Antoine received his BSc and MSc in Physics from the Université de Franche-Comté, Besançon, France in, in 2009 and 2011, respectively, and obtained his PhD from the University of Auckland, New Zealand in 2015. He is currently a Research Fellow at the Optoelectronics Research Centre (ORC), working on nonlinear silicon photonics.

Yohann Franz: Yohann received a B.Sc. and M.Sc degree in physics from the Université de Franche-Comté in 2011 and 2013 respectively. He is currently a PhD student at University of Southampton working on material enhancement using laser annealing.

Callum G. Littlejohns: Callum G. Littlejohns completed his PhD in the field of Silicon Photonics at the Optoelectronics Research Centre, University of Southampton in March 2015, having previously obtained a First Class Honours degree in Electronic Engineering at the University of Surrey. He has now begun his career as a Research Fellow at Nanyang Technological University in Singapore, but remains part of the Silicon Photonics group as a visitor. He has a track record of excellence, having received multiple awards throughout his academic life, including the Information Overload category winner at the 2015 EPSRC ICT Pioneers Award and the runner-up prize in the Best Student Poster award at the 2014 Optoelectronics Research Centre Photonics Day. His work has been published in multiple peer-reviewed journals including Scientific Reports, a Nature Publishing Group journal. His work was also selected as a prestigious post-deadline paper at the IEEE Group IV Photonics conference in Paris, 2014. The work completed during Callum’s PhD has been protected by two separate patents, both fully supported by the University of Southampton.

Sakellaris Mailis: Mailis is an Associate Professor at the Optoelectronics Research Center (ORC), University of Southampton, U.K. He received his Ph.D. degree from the University of Crete—Foundation for Research and Technology Hellas (FORTH), Greece, in 1996, in the area of optical signal processing with photorefractive materials. He has been investigating laser based method for materials processing including photosensitivity of semiconducting oxides, chalcogenides and lead germanate glasses. In the last decade Sakellaris has pioneered research on laser-based methods for the formation of optical waveguides, domain engineering and micro-structuring of ferroelectric lithium niobate and the laser processing of amorphous semiconductors for photonic applications.

Anna C. Peacock: Anna C. Peacock is a Professor of Photonics within the Optoelectronics Research Centre (ORC) at the University of Southampton. She obtained her BSc and MSc in Physics from The University of Auckland (New Zealand) in 1999 and 2001, respectively, and her PhD from the ORC in 2004. In 2007 she was awarded a five-year Royal Academy of Engineering Research

Fellowship, following which she established the Nonlinear Semiconductor Photonics group, where the focus of the research is on the design and development of novel semiconductor waveguides. She is a fellow of The Optical Society (FOSA) and the Institute of Physics (FInstP) and currently holds an EPSRC research fellowship.

David J. Thomson: David Thomson is a Royal Society University Research Fellow and Principal Research Fellow within the Silicon Photonics group of the Optoelectronics Research Centre. David leads research in the area of photonics for computing systems. His career in Photonics began with a year in industry at Nortel Networks in Paignton. David joined the University of Surrey in 2001 as an undergraduate student studying electronic engineering. He subsequently undertook PhD studies under the guidance of Professor Graham Reed investigating optical switching devices in silicon. From 2008 he worked as a research fellow in the same research group on a number of projects and different optical devices in silicon although focusing mainly on high speed active devices and their integration with other photonic and electronic devices. David moved to the University of Southampton in 2012 David taking up the role of senior research fellow. David has published over 40 journal papers, 10 patent applications and around 100 conference papers in the area of silicon photonics. David has served on 4 conference committees including IEEE Group IV Photonics and SPIE Photonics West.

Graham T. Reed: Graham Reed is Professor of Silicon Photonics and Group Leader. He joined Southampton in 2012 from the University of Surrey, where he was Professor of Optoelectronics, and was Head of the Department of Electronic Engineering from 2006 to 2012. Reed is a pioneer in the field of Silicon Photonics, and acknowledged as the individual who initiated the research field in the UK. He established the Silicon Photonics Research Group at Surrey in 1989. The first Silicon Photonics company in the world, Bookham Technology Inc., was founded by Reed's PhD student, Dr Andrew Rickman, and adopted the research developed in the Group. The Silicon Photonics Group have provided a series of world leading results since its inception, and are particularly well known for their work on silicon optical modulators. Reed is a regular invited and contributing author to the major Silicon Photonics conferences around the world. He has served on numerous international conference committees. He is currently a member of 5 international conference committees, and has published over 350 papers in the field of Silicon Photonics.